2016

From metal-organic frameworks to porous carbons: heterogeneous catalysis by carbon-supported Pd nanoparticles

Daniel Tesfagaber
Iowa State University

From metal-organic frameworks to porous carbons: Heterogeneous catalysis by carbon-supported Pd nanoparticles

by

Daniel Tesfagaber

A thesis submitted to the graduate faculty

in partial fulfillment of the requirements for the degree of

MASTER OF SCIENCE

Major: Chemistry

Program of Study Committee:
Wenyu Huang, Major Professor
Javier Vela
Yan Zhao

Iowa State University

Ames, Iowa

2016

TABLE OF CONTENTS

Page

ACKNOWLEDGEMENTS

I would like to thank my advisor, Prof. Wenyu Huang for his guidance and advice over the past few years. Thank you for encouraging me to try new ideas and to do many reactions. I would also like to thank my other committee members Dr. Javier Vela and Dr. Yan Zhao for supporting me throughout my research.

Thank you to all the members of the Huang research group. I would like to thank Dr. Chaoxian Xiao for his help and advice on my projects, and for patiently teaching me how to troubleshoot instruments in our lab. A big thank you to Raghu and Jason for helping me characterize my samples with XRD and TEM. In addition, my time at Iowa State was definitely made more fun thanks to Malinda Reichert and Brad Schmidt, who helped balance my out-of-lab life by playing basketball and racquetball with me.

A special thanks to my parents, Ahferom and Lucia, for supporting me over the years, even from 7451 miles away. While most parents would keep their kids away from chemicals, you let me design and run my own Chemistry experiments when I was thirteen. I'd like to thank you for encouraging me to become a curious adventurer. Thank you to all my brothers for being there for me whenever I needed anything. I appreciate your love and support, and am grateful for the sacrifices you've all made.

ABSTRACT

The last decade has seen a significant increase in research on biomass conversion to fuels and chemicals to address the limited supply of fossil fuels and to mitigate global warming. Numerous reactions and processes have been explored to upgrade biomass-derived platform chemicals to value-added products. The search for recyclable heterogeneous catalysts that remain stable and selective to desired products remains a key component for effective utilization of biomass. This thesis describes the synthesis of ultrasmall palladium nanoparticles supported on porous carbon derived from a sacrificial Al-MIL-101-NH_2 metal-organic framework (MOF) template. Although three different Pd precursors were examined, potassium tetrachloropalladate (II) was found to yield the smallest monodisperse Pd nanoparticles. The synthesized Pd catalyst was found to have excellent activity, recyclability and selectivity for the selective hydrogenation of furfural to furfuryl alcohol in mild conditions. Compared to industrial conditions, our catalyst required much lower temperature and pressure, and showed no sign of leaching of active Pd species.

Finally, we also attempted to synthesize intermetallic compounds by using this model system, but we were not able to achieve monodisperse nanoparticles. With further screening and testing, this simple method however still holds promise for the development of new carbon-supported catalysts which can be utilized for the transformation of platform biomass feedstocks to value-added products.

.

CHAPTER 1: INTRODUCTION

General Introduction

This thesis describes a process for the synthesis of ultrasmall and monodisperse palladium nanoparticles by using metal-organic frameworks (MOFs) as sacrificial templates. Porous MOFs have high surface areas, permanent nanoscale cavities, and open channels, which make them suitable to host small guest molecules [1]. Although MOFs have demonstrated potential applications as supports for metal nanoparticles (MNPs) in heterogeneous catalysis [2], they lack the chemical and mechanical robustness of traditional supports such as zeolites and silica, and thus start to break down in harsh reaction conditions. Also, leaching out of supported nanoparticles may occur and lead to decreased activities with subsequent catalyst recycling. However, it is possible to thermally decompose MOFs in the presence of guest metal precursors to produce well-dispersed MNPs on porous carbon nanocomposites (Figure 1). In this work, we use a direct solid-to-solid transformation where palladium precursors are initially dispersed inside the cavities of Al-MIL-101-NH_2 and then heated at high temperature (550°C in 10% H_2 in Ar gas flow for 4 h. See Experimental) to obtain Pd NPs@carbonized Al-MIL-101-NH_2 (denoted as Pd@C-Al-550). The effect of different precursors for the fabrication of Pd@C-Al-550 was also investigated. The catalytic activity of the prepared catalyst was then studied for the selective hydrogenation of furfural in aqueous solution.

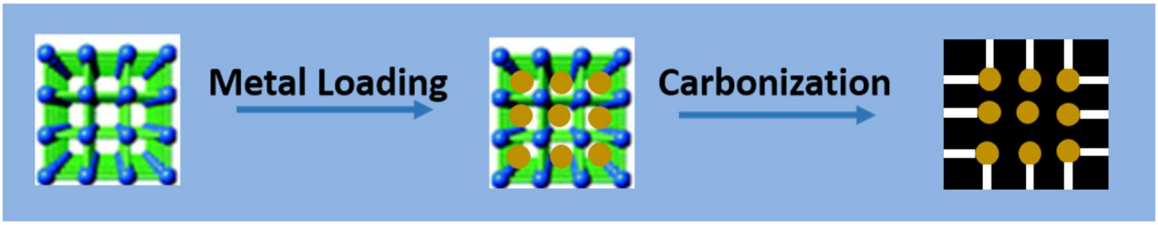

Figure 1. Preparation of Pd@Carbonized Metal-Organic Framework (Pd@C-MOF).

Biomass Conversion

Over the last decade, there has been renewed interest in finding a renewable source of carbon for fuels and chemicals. Since the beginning of the industrial age, the concentration of carbon dioxide in the atmosphere has risen with the increase of burning fossil fuels for energy [3]. It is estimated that over 90% of the world's transportation energy is currently derived from fossil fuel resources [4]. However, the consumption of fossil fuels for the production of energy and chemicals is associated with several well-documented issues. First, fossil fuels are finite resources which are being consumed with increasing demand by industrialized and emerging economies [5], potentially leading to depletion within the current century. Second, the use of fossil fuels contributes to increased emissions of CO_2 into the atmosphere, leading to weather disruptions [6] and global warming [7]. Thus, there is increased drive by governments and companies to substitute fossil fuel stocks with renewable carbon sources to support global economies with sustainable and renewable energy sources. To address these urgent concerns, solar, wind, hydroelectric, geothermal, and biomass energy sources are expected to play a significant role in the phasing out of fossil fuels in favor of greener energy sources.

Biomass has attracted a great deal of attention for its promising potential as a renewable source of carbon. Unlike fossil fuels, biomass derived fuels and chemicals are considered to be carbon neutral as any CO_2 produced is consumed by subsequent biomass growth [8]. In terms of their chemistry, while petroleum is composed mostly of hydrocarbons (linear and cyclic alkanes, alkenes, aromatics etc.), biomass is a mixture of highly functionalized oxygenated compounds embedded in complex polymeric structures [9]. Over the last century, the petrochemical industry has developed optimized methods to produce fuels by separation of hydrocarbons and/or subsequent catalytic upgrading. However, the transformation of biomass into fuels requires numerous chemical changes and further multistep processes [10]. Typical catalysts for petrochemical processes are designed to withstand high temperatures and hydrophobic environments, and are thus not suited to function effectively in processes which typically remove oxygen-containing functionality required for biomass upgrade[11].

The transformation of biomass into fuels and chemicals typically involves three catalytic routes: pyrolysis [12], gasification [13], and hydrolysis [14]. Pyrolysis and gasification generally convert whole biomass into upgradeable platforms such as syn-gas and bio-oil. Hydrolysis, on the other hand, involves complex processes that break down lignocellulose, a major component of biomass, into constituent parts. Lignin, a component of lignocellulose, is composed of a methoxylated phenylpropane that gives structural rigidity to plants. The other two major components, hemicellulose and cellulose, make up 25-35% and 40-50% respectively, of plant material. Cellullose is formed from β-glycosidic bonds linking glucose units into

polymers. Hemicellulose is composed of C_5 and C_6 sugar monomers such as D-galactose, D-manose, and the most abundant component – xylose. The transformation of these feedstocks requires subsequent modifications of a set of derivate platform molecules. The US Department of Energy in 2004 released a list of "Top 10 chemicals" deemed as platform molecules based on several indicators such as availability for its production and ease of transformation into fuels and chemicals [15]. These important platform molecules or building blocks are relatively simple compounds containing multiple functionalities in their structures and are suitable for various chemical transformations to valuable compounds. Some examples of important biomass platform molecules include sugars (glucose, xylose), polyols (xylitol, glycerol), furans (hydroxymethylfurfural, furfural) and acids (lactic acid, levulinic acid). A variety of hydrocarbon fuels and chemical intermediates can be produced by employing various types of reactions such as dehydration [16], isomerization [17], C-C coupling [18], hydrogenation [19], and hydrogenolysis [20]. Some of these reactions (e.g., hydrogenation and hydrogenolysis) are useful for oxygen removal, which is necessary for the requisite deoxygenation of biomass derivatives. Because the chemical composition of biomass derivatives is quite different from the final products, multiple controlled catalytic steps are typically required in such transformations.

In a typical strategy for the production of fuels and chemicals from lignocellulosic biomass, the biomass is first treated by using thermal [21], enzymatic [22], and/or chemical [23] and catalytic methods [24] to produce functional intermediates. Catalytic conversion methods allow for much milder processing

conditions compared to thermal methods, and allow for more tailored range of products. A pretreatment step removes the hemicellulose and some lignin from the biomass. The remaining cellulose fraction of the biomass is hydrolyzed to produce glucose or platform chemicals such as levulinic acid or 5-hydroxymethylfurfural (HMF). The lignin can be combusted for heat, or upgraded using catalysts to aromatic compounds and solvents. The hemicellulose stream can be upgraded to other platform chemicals, such as furfural [25], which itself can be upgraded to a variety of products [26].

Upgrading of Furfural to Furfuryl Alcohol

Furfural is a heterocyclic unsaturated aldehyde synthesized from xylan, mainly by acid hydrolysis of agricultural or forestry wastes (Fig. 1). It is the only large-volume platform chemical produced (ca. 250,000 tonnes per year) from carbohydrates [27]. Conversion of furfural (FAL) in the presence of H_2 and metallic catalysts can lead to a complex reaction network. Among the possible products, furfuryl alcohol (FOL) is one of the most interesting and valuable compounds since it can be used for the production of resins [28], synthetic fibers [29], farm chemicals [30], foundry binders [31], adhesives [32], [24]and some fine chemicals products such as vitamin C, lysine and tetrahydrofurfuryl alcohol [24].

Furfuryl alcohol is manufactured by the hydrogenation of furfural in the liquid or vapor phases over copper-chromite catalysts [33], which can cause environmental pollution due to the toxicity of Cr^{6+} ions [34]. Although other environmentally-friendlier catalysts have been explored, the conditions for hydrogenation are often at

high temperatures and high pressures (exceeding 473 K, 5 MPa, respectively) [35]. Other catalysts such as Raney nickel require further additives or modifiers such as heteropolyacid salts which make the catalyst recovery more complicated [36]. The need to selectively hydrogenate the carbonyl group while preserving the C=C bond also requires catalysts with modified surfaces [37]. Bimetallic Pt-Sn catalysts containing different amounts of tin show a high selectivity (>98%) to furfuryl alcohol [38]. Stevens et al. designed a switchable system based on a consecutive fixed-bed reactors loaded with copper chromite and Pd/C catalysts for the hydrogenation of furfural in supercritical CO_2 [39]. By controlling reaction conditions (temperature and H_2 concentration), this group was able to selectively produce furfuryl alcohol (97% yield), tetrahydrofurfuryl alcohol (96% yield), and furan (98% yield).

Palladium (Pd) Catalysts in Furfural Hydrogenation

The hydrogenation of furfural has been studied using different transition metal catalysts such as Co [40], Fe [41], Ni [37], Ru [42], Pd [43] and Pt [44]. Systems based on the non-metal catalysts, although successful in reaching 98% selectivity to the unsaturated alcohol – furfuryl alcohol, are disadvantageous as they suffer from poor recyclability, while other catalysts promote unwanted side reactions. Palladium (Pd) nanoparticles present a highly promising catalyst due to the relative low cost among precious metals, relative stability in the air and ease of recyclability. Different methods have been utilized to prepare Pd nanoparticles, such as atomic layer methods [45], wetness-impregnation [46], and decomposition of Pd-complexes [47]. Until now, only few studies have been reported using monometallic Pd nanoparticles

for the hydrogenation of furfural to furfuryl alcohol [48]. Zhao synthesized Pd/SiO_2 catalysts (with a mean size of 5 nm) from palladium nitrate precursor in mesoporous channels of SiO_2 to carry out furfural hydrogenation [49]. However, the reaction was carried out in an organic solvent (octane), whereby the best result achieved was 71% selectivity for furfuryl alcohol at 75% conversion of furfural. To the best of our knowledge, this is the only reported catalyst where Pd nanoparticles are utilized without the need for additional modifiers. In this thesis, I present a novel and facile method where Pd precursors preloaded into MOF cavities are first reduced into Pd nanoparticles upon carbonization, and at further higher temperature produce Pd NPs supported on a carbon matrix support (Pd@C-MOF). The activity of the catalyst was screened for the liquid phase hydrogenation of furfural in an aqueous phase, and the activities, compared to control catalysts are further discussed in this thesis.

CHAPTER 2: PALLADIUM NANOPARTICLES SUPPORTED ON CARBONIZED METAL-ORGANIC FRAMEWORKS

Abstract

Palladium nanoparticles supported on porous carbon matrix were synthesized by direct carbonization of Pd-impregnated metal-organic framework (MOF). The MOF cavity limits the growth of Pd NPs and serves to stabilize Pd nanoparticles, while the MOF itself serves as a template carbon source. The prepared catalyst has high catalytic activity for the selective hydrogenation of furfural and can be reused up to 9 times without any noticeable loss in activity.

Introduction

Metal-organic frameworks are a new class of crystalline compounds consisting of metal ions or clusters coordinated to organic linkers to form one- [50], two- [51], or three-dimensional pore structures [52]. The combination of organic and inorganic building blocks into highly ordered crystalline structures offers enormous flexibility in the tuning of the MOF's pore size, shape and structure. Furthermore, the high tunability offers great opportunities for functionalization, guest grafting, and encapsulation based on MOF platform. These materials also possess high adsorption capacities [53], specific surface areas [54], and pore volumes [55]. MOFs have emerged as candidate materials with considerable promise as heterogeneous catalysts. The two most common methodologies for MOF applications in catalysis take advantage of either metal coordination sites [56] or ligands (linkers) as active

sites [57]. Furthermore, by tuning parent linkers, MOFs can be post-synthetically modified to introduce new active sites [58].

A different approach that utilizes MOFs as heterogeneous catalysts consists of incorporation of guest species into the internal voids of the MOFs. Using this approach [59], various metal nanoparticles have been prepared exclusively inside the MOF matrices[60]. The confined spaces of MOFs not only act as stabilizing host materials, but also serve to limit particle growth and prevent agglomeration of MNPs. This approach often involves stepwise infiltration, followed by decomposition or reduction of the metal precursor molecules. By judicious choice of the host material, the sizes and shapes of the synthesized NPs can be controlled in the pores of the MOFs. A less common procedure to prepare MNPs is by simple grinding of organometallic complexes with MOFs, which could lead to formation of nanoparticles inside MOFs [61].

More recently, due to their high surface areas and tunable pores, MOFs have been successfully used as excellent templates for preparing mesoporous and microporous carbons [62]. This simple yet effective method utilizes primarily the controlled pyrolysis of sacrificial MOF templates, resulting in partially preserved long-range ordering and porosities in the carbonized MOF materials. In addition, by choosing suitable starting MOF templates, the incorporation of heteroatoms such as nitrogen into the carbon nanomatrix has been demonstrated, which showed enhanced mechanical [63] and energy-storage properties [64].

In this work, I combine the loading of Pd precursors into an amino-functionalized MOF and subsequent carbonization of the Pd-loaded MOF to prepare

ultrasmall Pd nanoparticles uniformly distributed throughout the resulting porous carbonaceous matrix. We examine the effects of Pd precursors on particle size, and different loading strategies to prepare small and monodisperse nanoparticles on the final carbon matrix. Finally, we screen the activity of these catalysts in the selective hydrogenation of furfural to furfuryl alcohol in an aqueous media. Owing to the high thermal stability of such nanocarbons, our method can be extended to prepare other MNPs or intermetallic compounds which are more difficult to prepare by traditional methods, in a more convenient way to prepare other heterogeneous catalysts.

Results and Discussion

Palladium (Pd) nanoparticles have previously been synthesized on different MOFs using several approaches [65]. We chose an aluminum (Al) metal-organic framework, Al-MIL-101-NH_2 [66] based on its high thermal stability (up to 370°C in air) and large surface area (BET 2100 $m^2\ g^{-1}$). Al-MIL-101-NH_2 is composed of supertetrahedral building units of rigid aminoterephthalate ligands and trimeric Al(III) octahedral clusters, possessing two types of quasi-spherical mesoporous cages formed by 12 pentagonal and 16 hexagonal faces, respectively. The medium cavities are accessible through 1.2 nm pentagonal windows, while the large cavities are connected through the same pentagonal windows and 1.6 nm hexagonal windows. Furthermore, the presence of the -NH_2 group was expected to uniformly decorate the resulting carbon matrix with N-atoms. The presence of N-atoms on carbon supports have previously been reported to improve the stability of MNPs such as Pt [67] and Pd [68] due to enhanced interaction between N atoms and the noble metal particles .

By starting with different palladium precursors, such as $Pd(OAc)_2$, $Pd(acac)_2$, and K_2PdCl_4, we find that the resulting Pd nanoparticles have varying average sizes (Table 1), with all three methods showing homogeneously distributed nanoparticles across the entire carbon matrix. From our experiments, we noted that the loading route had a notable effect on the resulting dispersion. For $Pd(OAc)_2$ and $Pd(acac)_2$, incipient wetness impregnation (volume of solvent less than total pore volume of MOF) of the precursors using methylene chloride or chloroform solvents resulted in a homogeneous yellow powder, which is indicative of a homogeneous dispersion of the precursors inside the MOFs (Figure 2). However, when either precursor is loaded using a wetness impregnation approach (volume of solvent significantly in excess of total pore volume of MOF), there were distinct areas of brown and yellow colors on the MOF, indicative of a non-uniform dispersion of Pd species on the MOF surface.

a.

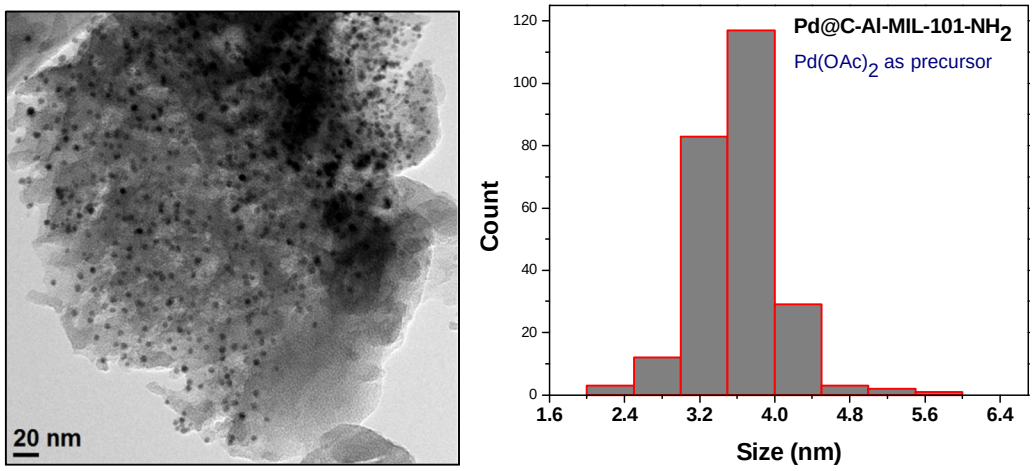

Figure 2. Representative TEM image and histogram Pd@C-Al-550 synthesized from (a) $Pd(OAc)_2$ (b) $Pd(acac)_2$ and (c) K_2PdCl_4.

b.

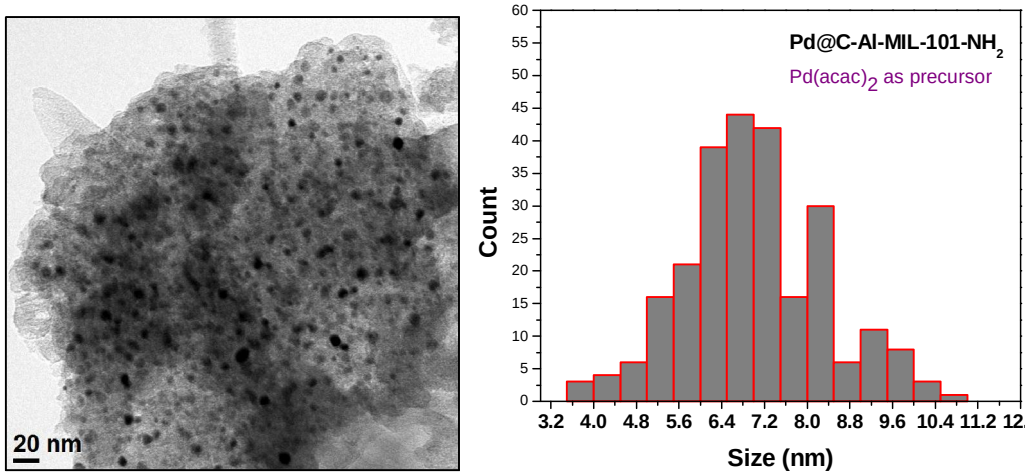

c.

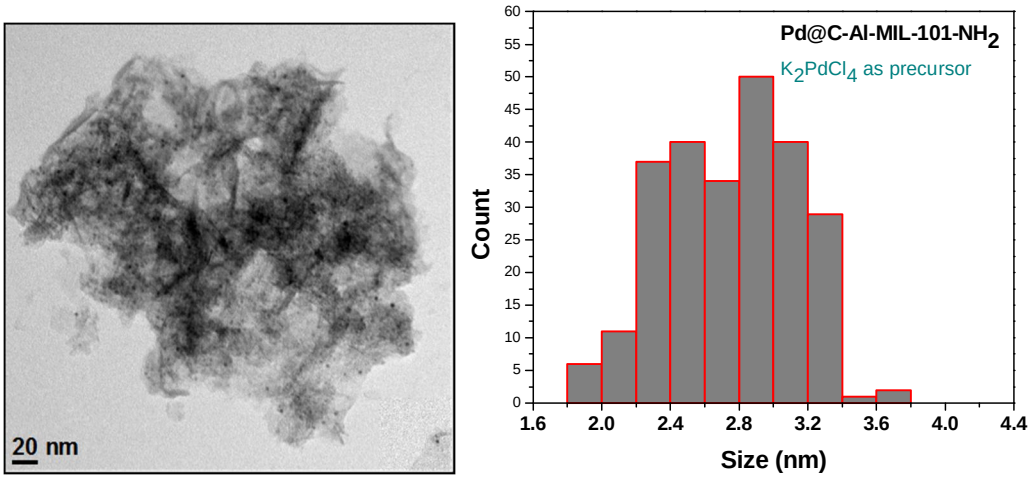

Figure 2 continued.

For the K_2PdCl_4 precursor, in contrast, due to its insolubility in organic solvents, the precursor was dispersed in water and only wetness impregnation resulted in a uniform distribution of Pd inside the MOF. Interestingly, the obtained carbon material (denoted as C-Al-550, where 550 denotes final carbonization temperature in °C), also resulted in different architectures as seen from TEM images.

Table 1. Precursor effect on size of Pd nanoparticles on carbonized Al-MIL-101-NH_2.

Pd Precursor	Solvent	Conditions	Pd diameter (nm)
$Pd(OAc)_2$	Methylene chloride	Incipient, r.t.	3.6 ± 0.5
$Pd(acac)_2$	Methylene chloride	Incipient	7.0 ± 1.3
K_2PdCl_4	Water	Wetness	2.7 ± 0.4

Based on TEM measurements, we find that the average particle size for Pd NPs is smallest (2.7 ± 0.4 nm) when K_2PdCl_4 is used as the precursor and loaded by incipient impregnation in water (Figure 3). To prove that the confinement by the MOF cage prevented Pd nanoparticle aggregation, we loaded Pd precursor salt into our MOF and reduced at only 200°C (see Experimental). It is observed that the average size of the Pd nanoparticles is clearly less than the cage sizes of the Al-MIL-101-NH_2 MOF (2.9 and 3.4 nm), possibly due to enhanced interaction between the -NH_2 groups on the linkers and Pd precursors. Although our group reported the enhanced loading Pt by the coordination of Pt ions with –NH_2 groups on a Zr-based MOF with amino-terephthalate linkers [69], we couldn't observe the same effect for Pd precursor with the linker on Al-MIL-101-NH_2. Additionally, we investigated the effect the MOF played in stabilizing and dispersing Pd precursors by reversing the sequence of metal loading and carbonization. That is, activated Al-MIL-101-NH_2 was first carbonized at high temperature (550°C) followed by loading of Pd precursors by either incipient wetness impregnation or wetness impregnation methods. Despite repeated attempts,

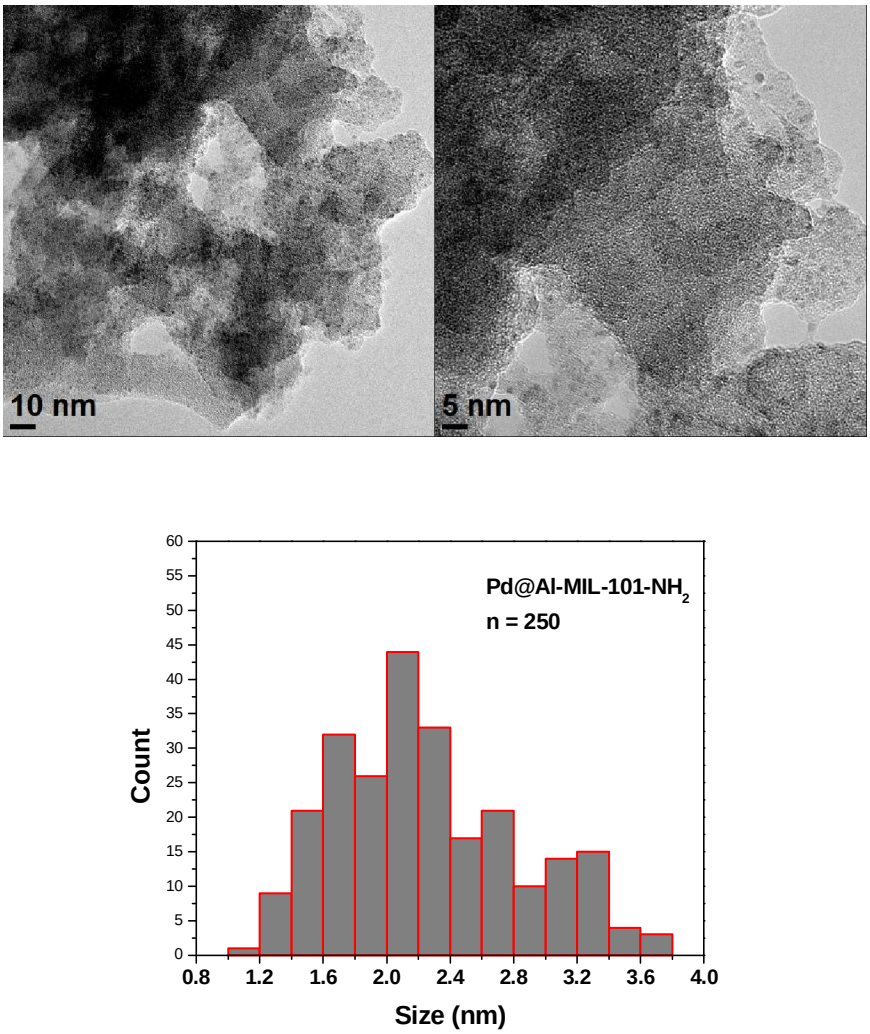

Figure 3. TEM image and histogram of Pd@Al-MIL-101-NH_2. Average particle size of Pd nanoparticles is 2.2 ± 0.6 nm. Pd loading is 3 wt. %.

we could not obtain uniformly distributed Pd nanoparticles inside our carbon matrix. This could result from the deposition of Pd ions on the surface of the carbonized MOF, which when reduced, freely move to form large aggregates of Pd nanoparticles (>40 nm), as evidenced by a representative TEM image below (Figure 4). For the carbonization process, we noted that all three samples underwent similar weight losses after carbonization, as summarized in Table 2.

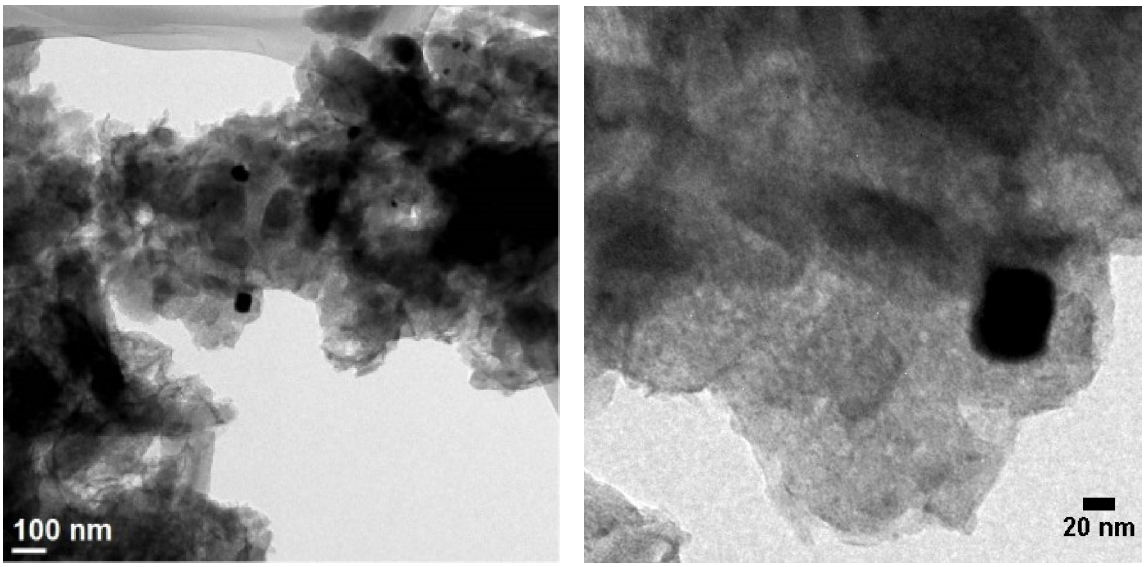

Figure 4. Pd NPs prepared by carbonization of Al-MIL-101-NH_2, followed by subsequent loading and reduction of Pd ions.

Table 2. Weight loss of Pd@Al-MIL-101-NH_2 after carbonization. Carbonization conditions: Ar gas flow, Ramping rate 1°C/min., 550°C for 4h, followed by natural cooling.

Pd Precursor	Loading Conditions	Wt. loss (%)
$Pd(OAc)_2$	Incipient, r.t.	64.7
$Pd(acac)_2$	Incipient	63.4
K_2PdCl_4	Wetness	66.2

Characterization of Pd@C-Al-550

Figure 5 shows powder X-ray diffraction (PXRD) patterns of Pd@C-Al-550, along with standard Pd reference patterns and a carbonized Al-MIL-101-NH_2 sample without any Pd loading. From XRD, we note that the prepared carbonized material, without Pd, C-Al-550 (green) showed broad peaks centered at 25 and 44°, which correspond to the respective (002) and (101) diffractions of graphitic carbon. For our

prepared Pd@C-Al-550 sample, characteristic peaks of Pd were also observed at 40, 47, 68 and 83°, corresponding to the (111), (200), (220) and (311) planes, respectively. Because the parent MOF, Al-MIL-101-NH_2, is composed of Al metal at the nodes, the presence of Al_2O_3 was expected from the treatment procedure. However, PXRD does not reveal any peaks possibly due to the presence of ultrasmall or amorphous Al_2O_3, as observed by Xu et al [70]. The presence of both metals is further confirmed by X-ray photoelectron spectroscopy (XPS) analysis.

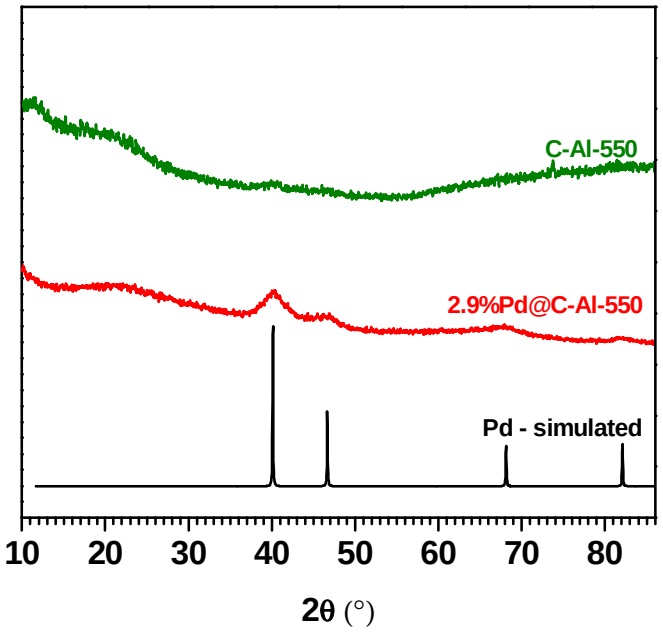

Figure 5. Powder XRD patterns of (a) C-Al-550 (green), (b)2.9%Pd@C-Al-550 (red), and (c) Pd simulated (black)

Figure 6 shows well-defined peaks at 334.7 and 339.9 eV which correspond to Pd $3d_{5/2}$ and $3d_{3/2}$ of metallic Pd. The XPS spectrum for Pd also shows that there are smaller intensity peaks for unreduced Pd^{2+} species in our sample, positioned at 336.1 and 341.3 eV, corresponding to Pd^{2+} $3d_{5/2}$ and $3d_{3/2,}$ respectively.

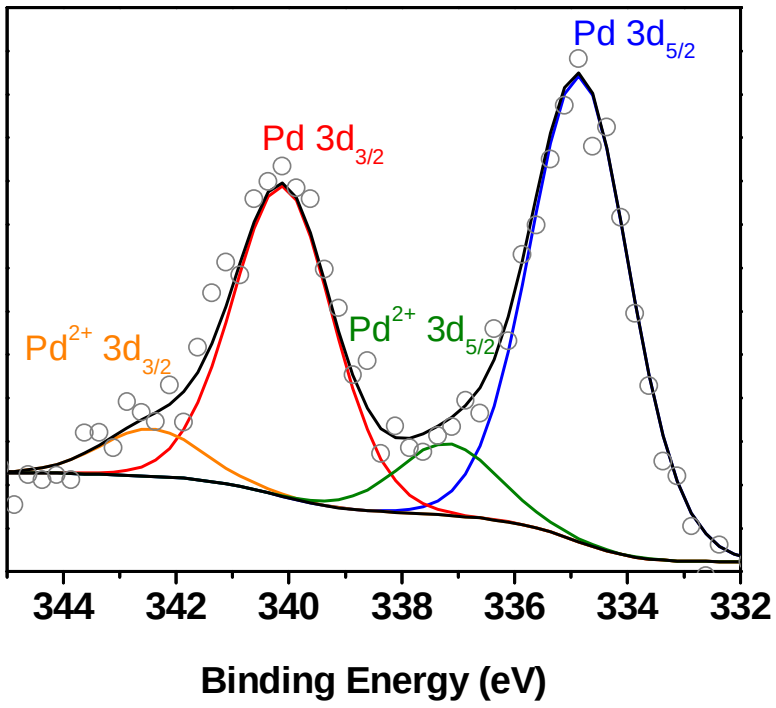

Figure 6. Pd XPS spectra of Pd@C-Al-550

It can also be seen that a peak for Al at a binding energy of 74.05 eV is observed for Al 2p (Figure 7), which is attributed to the presence of Al^{3+} species. This also confirms the presence of Al, which was not observed through XRD analysis.

The enlarged N 1s spectrum, as shown in Figure 8, indicates the presence of several peaks centered around 397.9, 399.7, and 401.7 eV [71]. The peak at 397.9 eV corresponds to pyridinic nitrogen atoms, that is, N bonded to two C atoms in a hexagon ring. The binding energy at 399.7 eV can be assigned to pyrrolic sp^2 nitrogen atoms bonded to carbon atoms. The highest binding energy at 401.7 eV is attributed to graphitic N atoms in a four membered ring [72]. Due to their electronegativity differences, the interaction of graphitic-N and C is proposed to cause permanent

polarization that enhances the wettability of the catalyst in water. Although pyridinic-N and pyrrolic-N species are present, their lone pairs do not favor the adsorption of

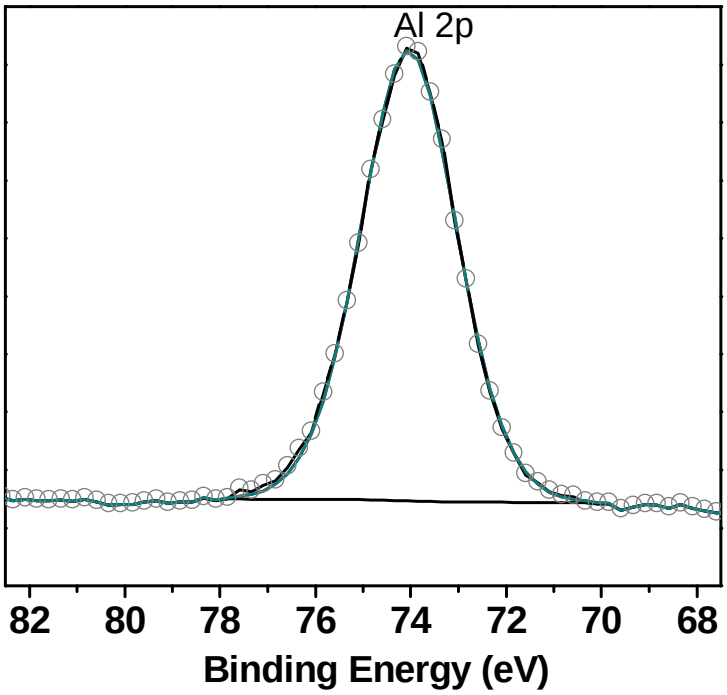

Figure 7. Al XPS spectra of Pd@C-Al-550

water molecules. The C 1s spectrum (Figure 9) can be deconvoluted into two peaks: the main intense peak at 284.5 eV (86.9%) assigned to graphitic sites, and a higher peak at 288.4 eV (13.13%) which are assigned to sp^3 C-C bond in aromatic rings [73]. The surface atomic composition of the carbonized catalyst is given in Table 4.

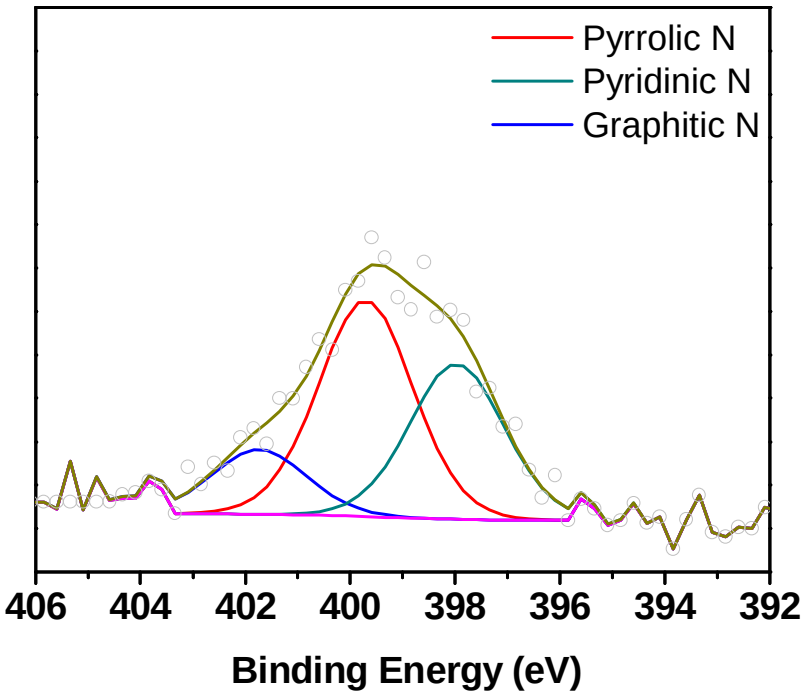

Figure 8. N XPS spectra of Pd@C-Al-550

Table 4. Surface composition of Pd@C-Al-550 as obtained from XPS analysis.

Catalyst	C%	N%	O%	Al%	Pd
Pd@C-Al-550	25.25	1.1	54.63	18.79	0.21

To determine the exact content of Pd and Al, inductively coupled plasma mass spectrometry (ICP-MS) measurements were carried out by first calcining the sample in air at high temperature, followed by digestion in aqua regia (see Experimental). We found out that Pd and Al in the carbonized samples were 2.9 and 36.1 wt. %, respectively.

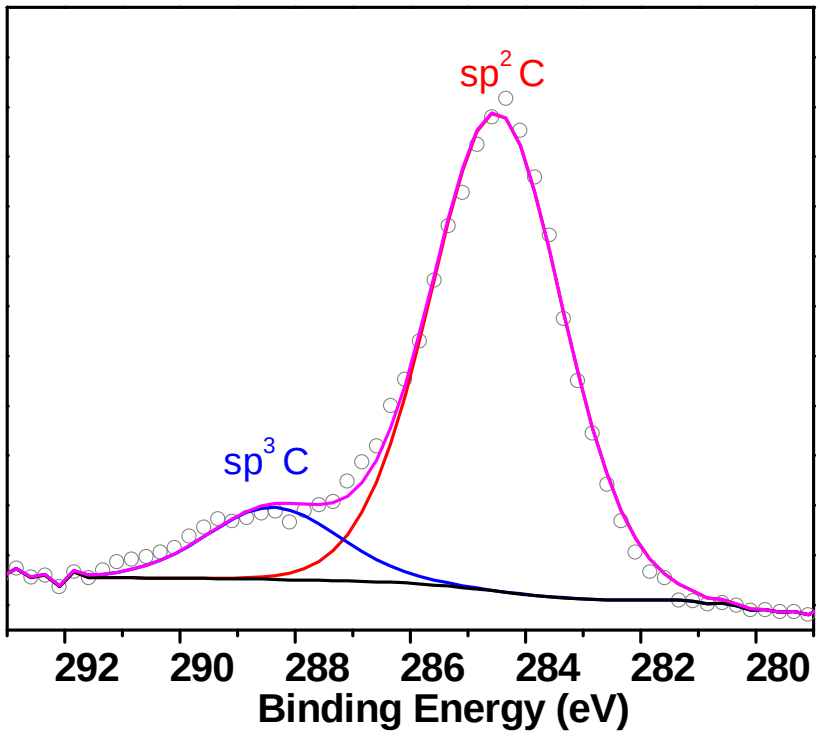

Figure 9. C XPS spectra of Pd@C-Al-550

N_2 adsorption-desorption isotherms of Pd@C-Al-550 shows the existence of different pore sizes ranging from micropores to macropores (Figure 10). At low relative pressures, the steep increase in the absorbed volume of N_2 shows the presence of micropores in the catalyst, while a desorption hysteresis at medium relative pressures indicates the presence of mesopores. At relative high pressures, the near vertical increase of relative pressures is attributed to the presence of macropores. The calculated BET surface area is 278 m^2 g^{-1} with distinct pore sizes of 3.7 and 11 nm, as shown from the BJH pore size distribution on Figure 11.

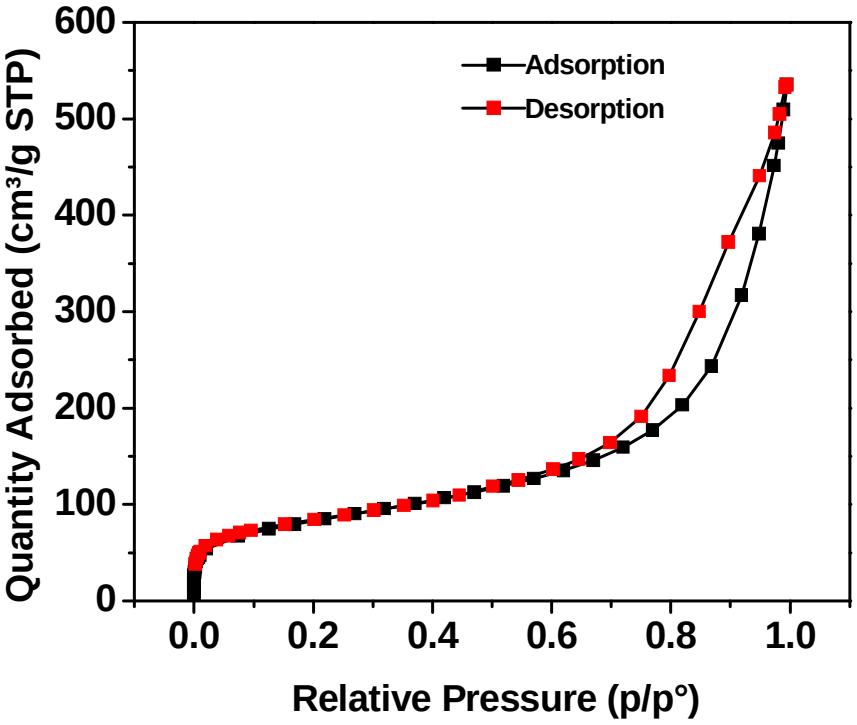

Figure 10. N_2 adsorption-desorption isotherm of 2.9%Pd@C-Al-550. BET Surface Area (278 m^2g^{-1}).

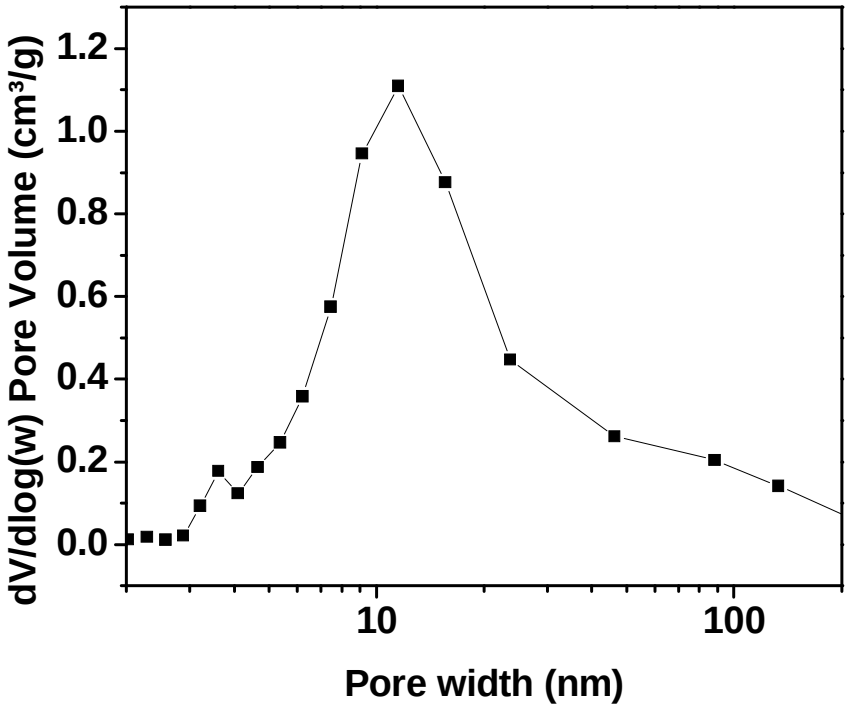

Figure 11. BJH pore size distribution of 2.9%Pd@C-Al-550

Furfural Hydrogenation to Furfuryl Alcohol

Numerous catalysts have been studied for the hydrogenation of furfural in liquid and vapor phase systems. Industrially, copper-chromite is used to convert furfural to furfuryl alcohol, usually at high temperatures and high pressures. Due to leaching and the toxicity of Cr metal, these catalysts are considered environmentally hazardous. Other noble metal catalysts, such as Pd and Ru have also been investigated for the selective hydrogenation to furfuryl alcohol, although they typically suffer from poor recyclability or the reaction is carried out in environmentally-unfriendly organic solvents. Furthermore, the temperatures and pressures are often quite high and result in the production of undesired over-hydrogenated by-products (Figure 12).

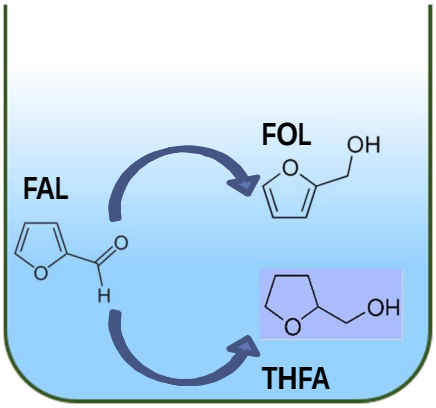

Figure 12. Hydrogenation of Furfural (FAL) into Furfuryl Alcohol (FOL) and Tetrahydrofurfuryl Alcohol (THFA).

Herein, we evaluate the performance of our catalyst for furfural hydrogenation in aqueous media. The result indicates that Pd@C-Al-550 efficiently catalyzes the reaction in mild conditions (4 MPa H_2, 60°C) with full conversion and excellent selectivity (100%) to furfuryl alcohol after only 2h (Figure 14). Although there are a

few studies on the selective hydrogenation of furfural in water [74], our results are far superior compared to the best reported catalysts [75]. We also halted the reaction after 0.5 h, to prove heterogeneity and absence of aggregation, and recycled up to 9 times, and observed high and consistent catalyst activity around 66% proving that the deactivation of the catalyst is not masked (Figure 13). This is a significant improvement since furfural is the product of acid catalyzed dehydration of pentoses proceeding in water [76]. The production of chemicals from furfural, an economic perspective, is highly beneficial when carried out in aqueous media as other organic solvents require further separation steps and are costly [77]. To further prove that the reaction was carried out by the heterogeneous catalyst, the reaction was stopped after 30 min., corresponding to a conversion of 65.7%, and the solid catalyst was then separated from the solution by centrifugation (Figure 15). The supernatant was then re-introduced into the reactor and the reaction was further carried out for another 90 min. Although there is a slight increase in the conversion, ICP-MS measurements show that there was no leaching of Pd or that Pd levels in the supernatant solution were at levels below detection limit of the instrument, suggesting there was strong interaction between Pd and the support. Comparison of TEM images of the catalyst before- and after- reaction show that the mean diameter of the Pd NPs increases only slightly from 2.5 nm to 2.7 nm after the 4th cycle of recyclability test (Figures 17 and 18, respectively).

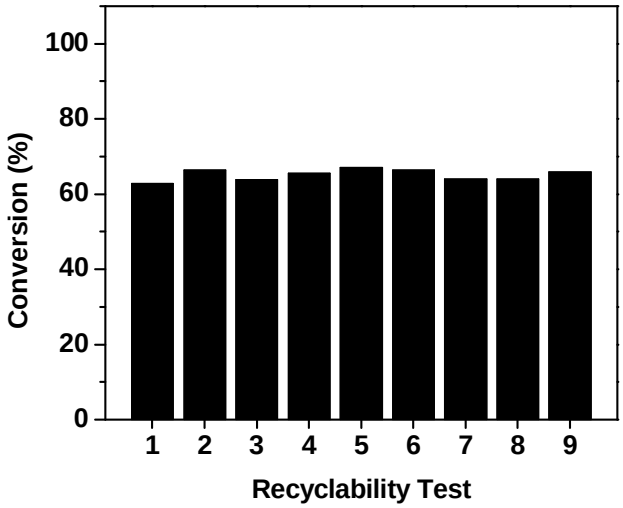

Figure 13. Recyclability test for Furfural hydrogenation. Reaction conditions: 4 mg of 2.9%Pd@C-Al-550, Pd:Furfural mol ratio (1:300), 3 ml of water, 4 MPa H_2, 60°C, reaction time of 0.5 h.

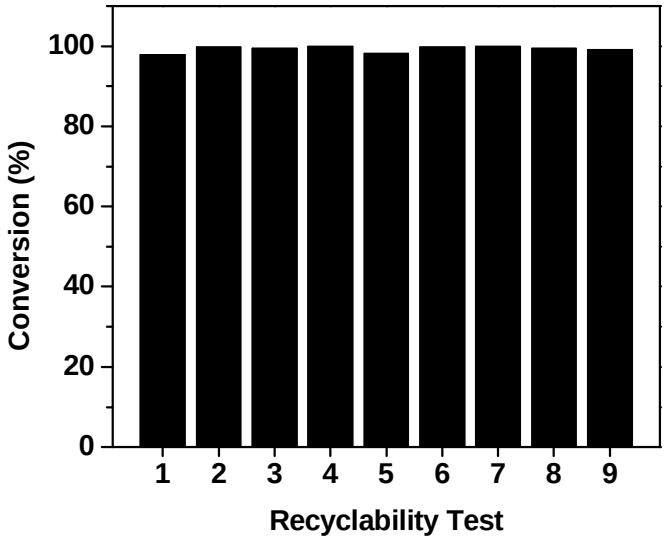

Figure 14. Recyclability test for furfural hydrogenation. Reaction conditions: 4 mg of 2.9%Pd@C-Al-550, Pd:Furfural mol ratio (1:300), 3 ml of water, 4 MPa H_2, 60°C, reaction time of 2 h.

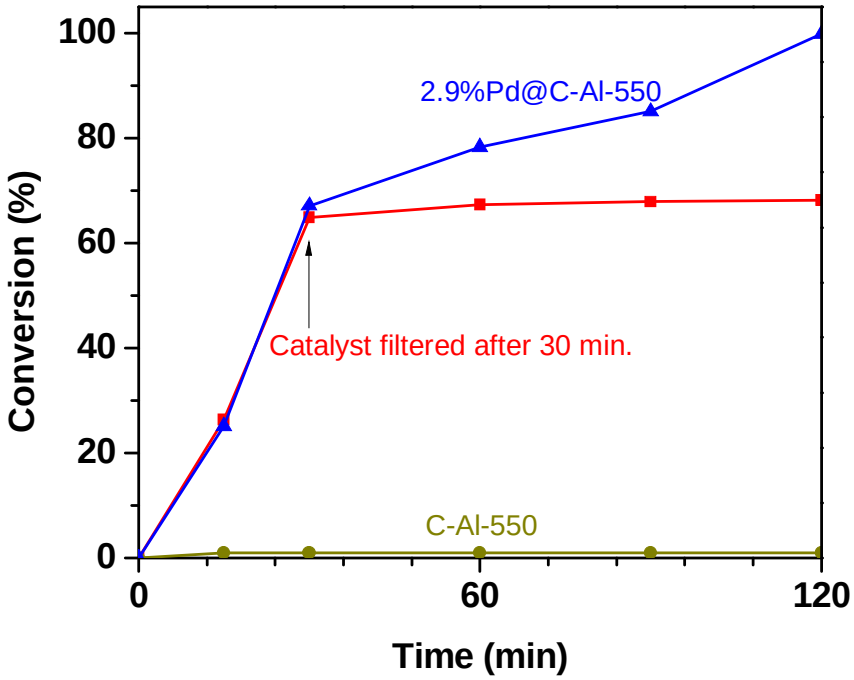

Figure 15. Leaching test for furfural hydrogenation. Reaction conditions: 4 mg of 2.9%Pd@C-Al-550, Pd:Furfural mol ratio (1:300), 3 ml of water, 4 MPa H_2, 60°C. Solid catalyst was filtered from the reaction after 0.5 h (red line) whereas an identical reaction was carried out in a separate vial without catalyst removal (blue line).

This is not surprising considering the fact that the reaction is carried out in a high pressure hydrogen atmosphere, possibly hydrogenating further Pd^{+2} species into metallic Pd in situ and leading to the slight particle size increase. To further compare our catalyst's performance versus control catalysts, Pd/C commercial catalyst (Sigma-Aldrich), Pd/alumina, and Pd@Al-MIL-101-NH_2 were also tested under the same reaction conditions. Although unfunctionalized Al-MIL-101 would have been a choice control catalyst due to the absence of amine functional groups, using similar synthesis conditions for Al-MIL-101-NH_2 only resulted in the formation of MIL-53(Al). However, to show that N-atoms in the carbonized catalyst increase wettability, we dispersed carbonized Al-MIL-101-NH_2 and Al-MIL-53 in water under ultrasonication for 30 min. It is clear that carbonized Al-MIL-101-NH_2 is

homogeneously dispersed in the solution, which may result in increased activity of our catalyst (Figure 16), while carbonized Al-MIL-53 does not disperse very well. The results of our control catalysts show that, although Pd/C and Pd@C-Al-550 have comparable activities (Table 5), Pd/C yields not only the desired furfuryl alcohol product but also the fully hydrogenated tetrahydrofurfuryl alcohol, a consequence of having multiple unsaturated sites on the substrate. In contrast, the Pd@C-Al-550 catalyst was shown to be selective only towards furfuryl alcohol, with a carbon balance of 92%. The recyclability of the catalyst was also found to be excellent, with conversion exceeding 99% obtained after 9 cycles under the same reaction conditions.

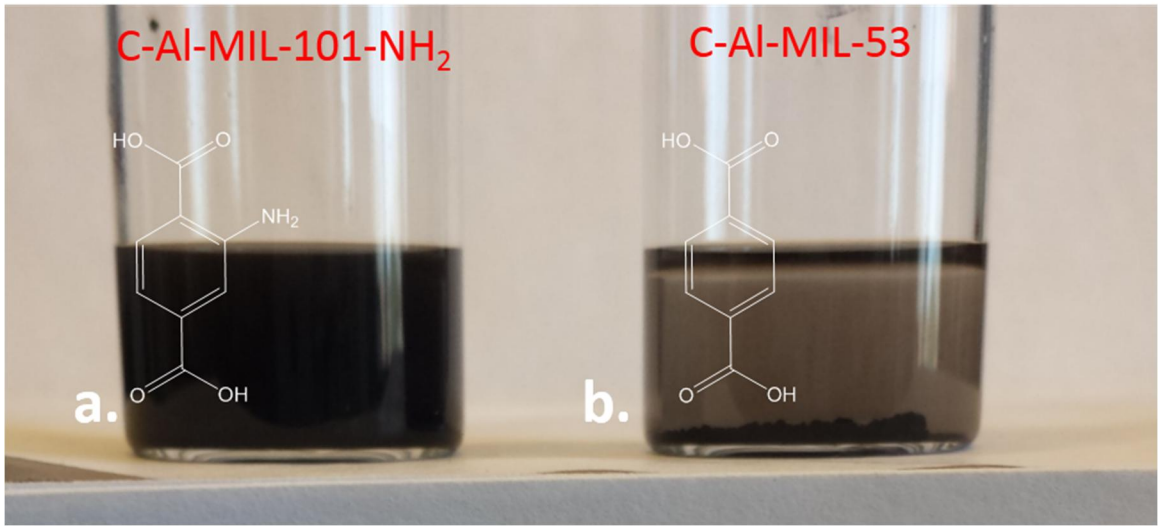

Figure 16. Wettability of carbonized (a) Al-MIL-101-NH_2 and (b) Al-MIL-53. Carbonization conditions: 550°C for 4 h under 10% H_2 in Ar gas flow. Both samples dispersed in water and ultrasonicated for 30 min.

Table 5. Comparison of Pd catalysts for furfural hydrogenation. Reaction conditions: 4 mg of Pd catalyst, Pd:Furfural mol ratio (1:300), 3 ml of water, 4 MPa H_2, 60°C, reaction time of 0.5 h.

Catalyst	Run	Conv.	Selectivity	
			FOL	THFA
2.9%Pd@C-Al-550	1	62.8	99.9	-
	2	66.4	99.9	-
	3	63.9	99.9	-
3.1%Pd@C-Al-750	1	55.6	99.9	-
	2	54.2	99.9	-
	3	57.5	99.7	-
Pd/C (Sigma-Aldrich)	1	62.4	79.4	20.6
	2	74.3	83.6	16.4
	3	73.2	74.9	25.1
	4	78.0	75.0	25
3%Pd@Al-MIL-101-NH_2	1	79.6	100	-
	2	23.9	100	-
Pd/Alumina (Sigma-Aldrich	1	12.0	41.3	58.7
	2	2.8	59.4	40.6
C-Al-550	1	0 / NA	0	-

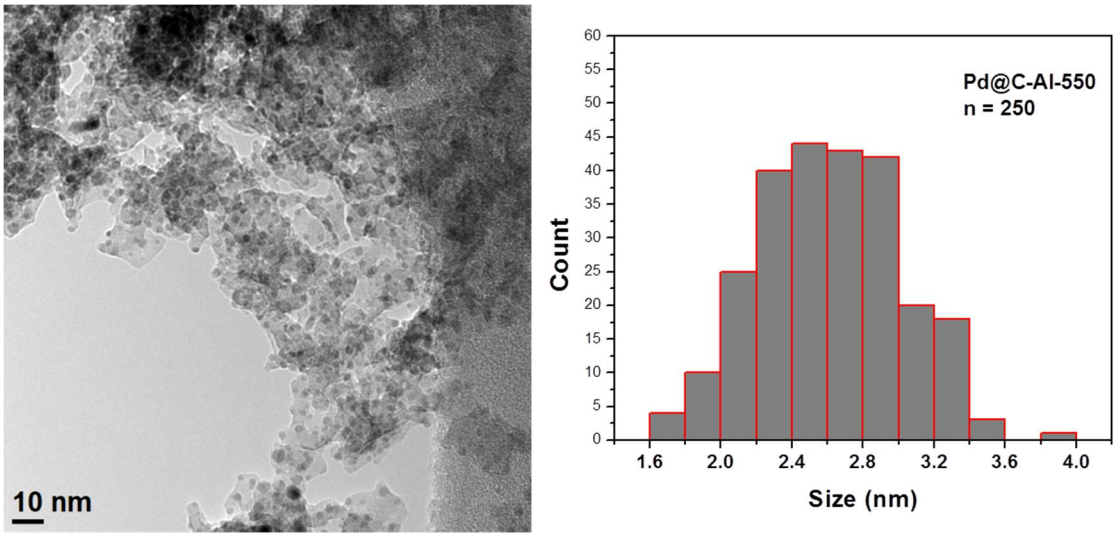

Figure 17. Bright field TEM image and histogram of fresh catalyst 2.9%Pd@C-Al-550. Average particle size of Pd nanoparticles is 2.5 ± 0.4 nm.

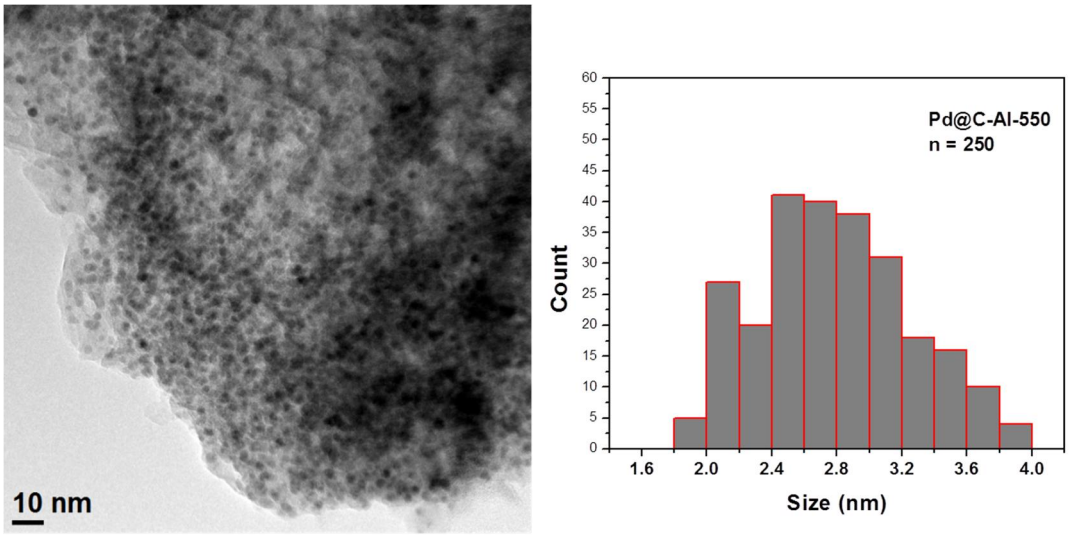

Figure 18. Bright field TEM image and histogram of 2.9%Pd@C-Al-550 after 4th recycle. Average particle size of Pd nanoparticles is 2.7 ± 0.5 nm.

Conclusions

We have shown a very simple and facile strategy to prepare Pd NPs supported on carbon supports by simple pre-loading of Pd precursors in well-defined MOFs,

followed by controlled carbonization. By using different precursors, we were able to obtain ultrasmall Pd nanoparticles with excellent dispersion across the carbon matrix. The presence of nitrogen in the MOF linker also enhances the uniform dispersion and stabilization of the resulting Pd NPs. Our results show that Pd nanoparticles prepared by the carbonization of Al-MIL-101-NH_2 are highly selective towards the aqueous phase hydrogenation of furfural to furfuryl alcohol. Furthermore, the reaction was carried out in very mild conditions and in an aqueous medium, which is ideally suited as it simulates industrial conditions. Our catalyst was easily recoverable and maintains its excellent activity and selectivity after 9 runs. In summary, this work offers new routes for the preparation ultrasmall monometallic and intermetallic nanoparticles supported on MOF-derived carbons as highly active heterogeneous catalysts.

Methods

Materials. Aluminum chloride hexahydrate ($AlCl_3.6H_2O$, 99%), 2-amino terephthalic acid (HO_2C-$C_6H_3NH_2$-CO_2H, 99+%), and potassium tetrachloropalladate (K_2PdCl_4, min. 32.0%Pd) were purchased from Acros Organics. Palladium (II) acetylacetonate ($Pd(acac)_2$, 99%) was purchased from Sigma-Aldrich. Palladium (II) acetate ($Pd(OAc)_2$, 98%) was purchased from Oakwood Chemical. N,N-dimethylformamide ($(CH_3)_2NCHO$, ACS grade) was purchased from Macron Fine Chemicals. Palladium on carbon (5% wt.) was purchased from Tokyo Chemical Industry (TCI). Palladium on alumina (5% wt.) was purchased from Aldrich. Materials were used as received.

Synthesis of Al-MIL-101-NH_2. The Al-MIL-101-NH_2 metal-organic framework precursor was synthesized by a previously reported literature procedure. In a typical synthesis, $AlCl_3.6H_2O$ (0.51g), 2-amino terephthalic acid (BDC-NH_2, 0.56g) and N,N-dimethyl formamide (DMF, 30mL) were placed in a Teflon-lined autoclave and sonicated until all reactants dissolved. The autoclave was then heated for 72 h at 403 K in an oven under static conditions. The resulting yellow powder was separated by centrifugation and washed with acetone three times (30 mL), and refluxed in ethanol for 16 h to remove organic species trapped within the pores. Then, the as-prepared MOF was slowly air-dried for 24 h and it was later activated at 120°C under vacuum (30 mTorr) for 6 h.

Synthesis of Pd@Al-MIL-101-NH_2. K_2PdCl_4 precursor: Al-MIL-101-NH_2 (200 mg) was dispersed in 15 ml of ultrapure water. After sonication for 30 min., an aqueous solution of potassium tetrachloropalladate (II) (6.31 mg K2PdCl4 in 3 mL of water) was added dropwise to the MOF solution under vigorous stirring in an oil bath preset at 40°C. After 24 h of stirring, the as-prepared Pd^{+2} impregnated MOF was washed three times every 12 h with fresh ultrapure water. The obtained sample was slowly air-dried for 24 h and activated at 120°C under vacuum (30 mTorr) for 6 h. $Pd(OAc)_2$ and $Pd(acac)_2$ precursors: A calculated amount (1% wt. Pd in MOF) of palladium acetate (Pd(OAc)2) was dissolved in chloroform (0.12 mL) and added drop wise to a freshly activated Al-MIL-101-NH_2 (200 mg) under continuous stirring at room temperature. After 30 min., the obtained mixture was slowly air-dried for 12 h and activated at 100°C under vacuum (30 mTorr) for 6 h. A similar procedure was followed for the palladium acetylacetonate precursor.

Synthesis of Pd@C-Al-X (where x denotes the final carbonization temperature). The activated Pd@Al-MIL-101-NH_2 samples were placed into a quartz boat, which was put in the middle of a quartz tube in a furnace and charged with Argon gas on one-end for 30 min. to flush air out. Then, the furnace was gradually heated to the desired final temperature (55O°C, 650°C, 750°C) at a rate of 1°C/min. under a 50 mL/min flow of 10% H2/Ar. After maintaining the final temperature for 4 h, the sample was allowed to cool naturally to room temperature and the obtained black powder was stored in sealed vials until further use.

Furfural Hydrogenation

In a typical batch experiment, 4 mg of the catalyst was dispersed in 3 ml of ultrapure water in a 20 ml glass vial equipped with a magnetic stirrer. The vial was sonicated for 1 min. to uniformly disperse the catalyst. Then, a calculated amount of furfural (Fisher Scientific), with Furfural:Pd ratio (300:1) was added into the solution. The vial was then sealed with a rubber cap equipped with a needle to aid H_2 diffusion. Then the vial was placed inside a Parr autoclave and flushed several times with H_2, and finally charged with 4 MPa H_2. The autoclave was loaded in an oil bath that was preheated at 60°C with magnetic stirring at 700 rpm for the designated time. After the reaction was finished, all the contents were analyzed using a gas chromatograph (GC) equipped with a HP-5 capillary column (30 m x 0.32 m x 0.25 μm) and a flame ionization detector. The products were identified by Agilent 6890N/5975 gas

chromatograph mass spectroscopy (GC-MS) equipped with a HP-5 ms capillary column (30 m x 0.25 mm x 0.25 μm) and a flame ionization detector.

Recycling Test. The catalyst was isolated at the end of the reaction and the liquid was separated by centrifugation. The solid catalyst was then washed three times with ethanol and dried in ambient air, followed by further drying at 50°C in an oven. The dried solid catalyst was reused for further recyclability tests in similar conditions as the first cycle.

Leaching Test. After a reaction time of 30 min, the reaction was stopped by removing the autoclave from the oil bath and releasing H_2 gas from the reactor. A 100 uL solution was taken from the reaction mixture to analyze using a gas chromatograph. The solid catalyst was separated from the solution and the reaction with the filtrate was further continued by placing the vial in the autoclave and recharging with 4 MPa H_2. This cycle was repeated until a final total reaction time of 120 min was attained.

Characterization *Powder X-ray diffraction* (XRD) was measured using Cu Kα radiation (40 kV, 40 mA, λ = 0.1541 nm). *Transmission electron microscopy* (TEM) The size and morphology of the samples were investigated by using transmission electron microscopy (TEM) on a Tecnai G2 F20 electron microscope. *Particle dimensions* were measured manually or with ImageJ for >250 particles per sample. Average sizes are reported ± standard deviations. Surface area analysis of the

catalyst was performed by nitrogen sorption isotherms using a Micrometrics 3Flex surface characterization analyzer at 77 K. *X-ray photoelectron spectroscopy* (XPS) measurements were performed using a PHI 5500 Multitechnique system (Physical Electronics, Chanhassen, MN) with a monochromatized Al Kα X-ray source (hν = 1486.6 eV). The binding energy values were determined using C 1s at 284.8 eV as a reference. *Inductively Coupled Plasma Mass Spectrometry (ICP-MS)* (X Series II, Thermo Scientific) was performed to determine the actual metal content of Pd and Al in the catalysts.

CHAPTER 3: CONCLUSIONS

In summary, we demonstrated a simple yet effective way of preparing metal nanoparticles (MNPs) supported on a hybrid carbon – metal oxide support by carbonization of a template metal-organic framework. By carefully impregnating Al-MIL-101-NH_2 with various palladium (Pd) precursors, we were able to obtain homogeneously dispersed ultrasmall Pd nanoparticles with various average particles sizes. From our results, we determined that K_2PdCl_4 was the best precursor to obtain the smallest Pd nanoparticles, with an average particle size of 2.7 nm.

To determine the activity of our heterogeneous catalyst, we screened our catalyst for the selective hydrogenation of furfural. Compared to industrial catalysts, our catalyst exhibited excellent activity and selectivity towards furfuryl alcohol, a highly desirable intermediate used for the production of resins, adhesives, fibers, and some fine chemicals such as Vitamin C and tetrahydrofurfuryl alcohol. Furthermore, the reaction was carried out suitably in water, mimicking conditions in industry, and in relatively low temperature and pressure. Finally, we were able to recover and recycle our catalyst for up to 9 cycles without any significant decrease in activity.

Research on metal organic-framework (MOF) catalysis is still a relatively new area of heterogeneous catalysis. The excellent tunability and functionalities of MOFs makes MOFs promising candidates in the area of catalysis. Furthermore, as we have shown in this work, MOFs can also be used as templates for new functional materials such as porous carbons. By judiciously choosing template MOFs with a desired attribute, for example, the presence of heteroatoms or specific cage sizes, metal

nanoparticles of different sizes can be supported on a heteroatom-decorated porous carbon matrix by a careful carbonization treatment. This method may pave the way for other more complex structures such as bimetallic alloys or intermetallic compounds supported on porous carbons or on metal-oxide carbon hybrid structures. Future studies will be directed towards the controlled synthesis of other nanoparticles and intermetallic compounds which are more useful in biomass upgrade to fuels and fine chemicals.

REFERENCES

[1] K. Kim, Metal-organic frameworks: Entering the recognition domain, Nat Chem 1 (2009) 603-604.

[2] X. Li, Z. Guo, C. Xiao, T.W. Goh, D. Tesfagaber, W. Huang, Tandem Catalysis by Palladium Nanoclusters Encapsulated in Metal–Organic Frameworks, ACS Catalysis 4 (2014) 3490-3497.

[3] S. Manabe, R.J. Stouffer, Multiple-century response of a coupled ocean-atmosphere model to an increase of atmospheric carbon dioxide, Journal of climate 7 (1994) 5-23.

[4] P. Börjesson, Energy analysis of biomass production and transportation, Biomass and Bioenergy 11 (1996) 305-318.

[5] G. Marland, T. Boden, R. Andres, A. Brenkert, C. Johnston, Global, regional, and national fossil fuel CO2 emissions, Trends: A Compendium of Data on Global Change (2007) 37831-36335.

[6] P.M. Cox, R.A. Betts, C.D. Jones, S.A. Spall, I.J. Totterdell, Acceleration of global warming due to carbon-cycle feedbacks in a coupled climate model, Nature 408 (2000) 184-187.

[7] S. Solomon, G.-K. Plattner, R. Knutti, P. Friedlingstein, Irreversible climate change due to carbon dioxide emissions, Proceedings of the national academy of sciences (2009) pnas. 0812721106.

[8] G. Zanchi, N. Pena, N. Bird, Is woody bioenergy carbon neutral? A comparative assessment of emissions from consumption of woody bioenergy and fossil fuel, GCB Bioenergy 4 (2012) 761-772.

[9] F.-X. Collard, J. Blin, A review on pyrolysis of biomass constituents: Mechanisms and composition of the products obtained from the conversion of cellulose, hemicelluloses and lignin, Renewable and Sustainable Energy Reviews 38 (2014) 594-608.

[10] J.C. Serrano-Ruiz, R. Luque, A. Sepulveda-Escribano, Transformations of biomass-derived platform molecules: from high added-value chemicals to fuels via aqueous-phase processing, Chemical Society Reviews 40 (2011) 5266-5281.

[11] A. Corma, S. Iborra, A. Velty, Chemical routes for the transformation of biomass into chemicals, Chemical reviews 107 (2007) 2411-2502.

[12] D. Mohan, C.U. Pittman, P.H. Steele, Pyrolysis of wood/biomass for bio-oil: a critical review, Energy & fuels 20 (2006) 848-889.

[13] L. Wang, C.L. Weller, D.D. Jones, M.A. Hanna, Contemporary issues in thermal gasification of biomass and its application to electricity and fuel production, Biomass and Bioenergy 32 (2008) 573-581.

[14] J.B. Binder, R.T. Raines, Fermentable sugars by chemical hydrolysis of biomass, Proceedings of the National Academy of Sciences 107 (2010) 4516-4521.

[15] T. Werpy, G. Petersen, A. Aden, J. Bozell, J. Holladay, J. White, A. Manheim, D. Eliot, L. Lasure, S. Jones, Top value added chemicals from biomass. Volume 1-Results of screening for potential candidates from sugars and synthesis gas, DTIC Document, 2004.

[16] J.N. Chheda, J.A. Dumesic, An overview of dehydration, aldol-condensation and hydrogenation processes for production of liquid alkanes from biomass-derived carbohydrates, Catalysis Today 123 (2007) 59-70.

[17] Y. Román-Leshkov, M. Moliner, J.A. Labinger, M.E. Davis, Mechanism of glucose isomerization using a solid Lewis acid catalyst in water, Angewandte Chemie International Edition 49 (2010) 8954-8957.

[18] E. F Iliopoulou, Review of CC coupling reactions in biomass exploitation processes, Current Organic Synthesis 7 (2010) 587-598.

[19] A.M.R. Galletti, C. Antonetti, V. De Luise, M. Martinelli, A sustainable process for the production of γ-valerolactone by hydrogenation of biomass-derived levulinic acid, Green Chemistry 14 (2012) 688-694.

[20] X. Chen, X. Wang, S. Yao, X. Mu, Hydrogenolysis of biomass-derived sorbitol to glycols and glycerol over Ni-MgO catalysts, Catalysis Communications 39 (2013) 86-89.

[21] W. Yan, T.C. Acharjee, C.J. Coronella, V.R. Vásquez, Thermal pretreatment of lignocellulosic biomass, Environmental Progress & Sustainable Energy 28 (2009) 435-440.

[22] H. Jørgensen, J.B. Kristensen, C. Felby, Enzymatic conversion of lignocellulose into fermentable sugars: challenges and opportunities, Biofuels, Bioproducts and Biorefining 1 (2007) 119-134.

[23] J.B. Binder, R.T. Raines, Simple chemical transformation of lignocellulosic biomass into furans for fuels and chemicals, J. Am. Chem. Soc. 131 (2009) 1979-1985.

[24] C.-H. Zhou, X. Xia, C.-X. Lin, D.-S. Tong, J. Beltramini, Catalytic conversion of lignocellulosic biomass to fine chemicals and fuels, Chemical Society Reviews 40 (2011) 5588-5617.

[25] S. Dutta, S. De, B. Saha, M.I. Alam, Advances in conversion of hemicellulosic biomass to furfural and upgrading to biofuels, Catalysis Science & Technology 2 (2012) 2025-2036.

[26] J.P. Lange, E. van der Heide, J. van Buijtenen, R. Price, Furfural—a promising platform for lignocellulosic biofuels, ChemSusChem 5 (2012) 150-166.

[27] D.T. Win, Furfural-gold from garbage, Au J Technol 8 (2005) 185-190.

[28] A. Patel, S. Soni, H. Patel, Synthesis, characterization and curing of o-cresol–furfural resins, International Journal of Polymeric Materials 58 (2009) 509-516.

[29] N. Reddy, Y. Yang, Biofibers from agricultural byproducts for industrial applications, TRENDS in Biotechnology 23 (2005) 22-27.

[30] A. Datta, S. Walia, B.S. Parmar, Some furfural derivatives as nitrification inhibitors, Journal of agricultural and food chemistry 49 (2001) 4726-4731.

[31] D.W. Akerberg, Catalyst system for furan resins, Google Patents, 1984.

[32] A. Pizzi, E. Orovan, F. Cameron, The development of weather-and boil-proof phenol-resorcinol-furfural cold-setting adhesives, Holz als Roh-und Werkstoff 42 (1984) 467-472.

[33] D. Vargas-Hernandez, J. Rubio-Caballero, J. Santamaría-González, R. Moreno-Tost, J. Merida-Robles, M. Perez-Cruz, A. Jimenez-Lopez, R. Hernandez-Huesca, P. Maireles-Torres, Furfuryl alcohol from furfural hydrogenation over copper supported on SBA-15 silica catalysts, Journal of Molecular Catalysis A: Chemical 383 (2014) 106-113.

[34] A.K. Shanker, C. Cervantes, H. Loza-Tavera, S. Avudainayagam, Chromium toxicity in plants, Environment international 31 (2005) 739-753.

[35] H. Luo, H. Li, L. Zhuang, Furfural Hydrogenation to Furfuryl Alcohol over a Novel Ni-Co-B Amorphous Alloy Catalyst, Chemistry Letters (2001) 404-405.

[36] L. Baijun, L. Lianhai, W. Bingchun, C. Tianxi, K. Iwatani, Liquid phase selective hydrogenation of furfural on Raney nickel modified by impregnation of salts of heteropolyacids, Applied Catalysis A: General 171 (1998) 117-122.

[37] S.-P. Lee, Y.-W. Chen, Selective hydrogenation of furfural on Ni-P, Ni-B, and Ni-PB ultrafine materials, Industrial & engineering chemistry research 38 (1999) 2548-2556.

[38] A.B. Merlo, V. Vetere, J.F. Ruggera, M.L. Casella, Bimetallic PtSn catalyst for the selective hydrogenation of furfural to furfuryl alcohol in liquid-phase, Catalysis Communications 10 (2009) 1665-1669.

[39] J.G. Stevens, R.A. Bourne, M.V. Twigg, M. Poliakoff, Real-time product switching using a twin catalyst system for the hydrogenation of furfural in supercritical CO2, Angewandte Chemie 122 (2010) 9040-9043.

[40] W. Xu, H. Wang, X. Liu, J. Ren, Y. Wang, G. Lu, Direct catalytic conversion of furfural to 1, 5-pentanediol by hydrogenolysis of the furan ring under mild conditions over Pt/Co 2 AlO 4 catalyst, Chemical Communications 47 (2011) 3924-3926.

[41] H. Li, H. Luo, L. Zhuang, W. Dai, M. Qiao, Liquid phase hydrogenation of furfural to furfuryl alcohol over the Fe-promoted Ni-B amorphous alloy catalysts, Journal of molecular catalysis A: Chemical 203 (2003) 267-275.

[42] A.S. Gowda, S. Parkin, F.T. Ladipo, Hydrogenation and hydrogenolysis of furfural and furfuryl alcohol catalyzed by ruthenium (II) bis (diimine) complexes, Applied Organometallic Chemistry 26 (2012) 86.

[43] S. Sitthisa, D.E. Resasco, Hydrodeoxygenation of furfural over supported metal catalysts: a comparative study of Cu, Pd and Ni, Catalysis letters 141 (2011) 784-791.

[44] J. Kijeński, P. Winiarek, T. Paryjczak, A. Lewicki, A. Mikołajska, Platinum deposited on monolayer supports in selective hydrogenation of furfural to furfuryl alcohol, Applied Catalysis A: General 233 (2002) 171-182.

[45] J. Elam, A. Zinovev, C. Han, H. Wang, U. Welp, J. Hryn, M. Pellin, Atomic layer deposition of palladium films on Al 2 O 3 surfaces, Thin Solid Films 515 (2006) 1664-1673.

[46] M. Sabo, A. Henschel, H. Fröde, E. Klemm, S. Kaskel, Solution infiltration of palladium into MOF-5: synthesis, physisorption and catalytic properties, Journal of Materials Chemistry 17 (2007) 3827-3832.

[47] H. Kosslick, I. Mönnich, E. Paetzold, H. Fuhrmann, R. Fricke, D. Müller, G. Oehme, Suzuki reaction over palladium-complex loaded MCM-41 catalysts, Microporous and mesoporous materials 44 (2001) 537-545.

[48] S.H. Pang, J.W. Medlin, Adsorption and reaction of furfural and furfuryl alcohol on Pd (111): Unique reaction pathways for multifunctional reagents, Acs Catalysis 1 (2011) 1272-1283.

[49] Y. Zhao, Facile synthesis of Pd nanoparticles on SiO2 for hydrogenation of biomass-derived furfural, Environmental chemistry letters 12 (2014) 185-190.

[50] J. Fan, H.-F. Zhu, T.-a. Okamura, W.-Y. Sun, W.-X. Tang, N. Ueyama, Novel one-dimensional tubelike and two-dimensional polycatenated metal-organic frameworks, Inorganic chemistry 42 (2003) 158-162.

[51] A. Kondo, H. Noguchi, L. Carlucci, D.M. Proserpio, G. Ciani, H. Kajiro, T. Ohba, H. Kanoh, K. Kaneko, Double-step gas sorption of a two-dimensional metal-organic framework, J. Am. Chem. Soc. 129 (2007) 12362-12363.

[52] D.N. Dybtsev, H. Chun, K. Kim, Three-dimensional metal–organic framework with (3, 4)-connected net, synthesized from an ionic liquid medium, Chemical communications (2004) 1594-1595.

[53] H. Li, M. Eddaoudi, M. O'Keeffe, O.M. Yaghi, Design and synthesis of an exceptionally stable and highly porous metal-organic framework, Nature 402 (1999) 276-279.

[54] H. Furukawa, N. Ko, Y.B. Go, N. Aratani, S.B. Choi, E. Choi, A.Ö. Yazaydin, R.Q. Snurr, M. O'Keeffe, J. Kim, Ultrahigh porosity in metal-organic frameworks, Science 329 (2010) 424-428.

[55] B. Chen, M. Eddaoudi, S. Hyde, M. O'keeffe, O. Yaghi, Interwoven metal-organic framework on a periodic minimal surface with extra-large pores, Science 291 (2001) 1021-1023.

[56] Y.K. Hwang, D.Y. Hong, J.S. Chang, S.H. Jhung, Y.K. Seo, J. Kim, A. Vimont, M. Daturi, C. Serre, G. Férey, Amine grafting on coordinatively unsaturated metal centers of MOFs: consequences for catalysis and metal encapsulation, Angewandte Chemie International Edition 47 (2008) 4144-4148.

[57] J. An, S.J. Geib, N.L. Rosi, High and selective CO2 uptake in a cobalt adeninate metal− organic framework exhibiting pyrimidine-and amino-decorated pores, J. Am. Chem. Soc. 132 (2009) 38-39.

[58] Z. Wang, S.M. Cohen, Postsynthetic modification of metal–organic frameworks, Chemical Society Reviews 38 (2009) 1315-1329.

[59] G. Lu, S. Li, Z. Guo, O.K. Farha, B.G. Hauser, X. Qi, Y. Wang, X. Wang, S. Han, X. Liu, Imparting functionality to a metal–organic framework material by controlled nanoparticle encapsulation, Nature chemistry 4 (2012) 310-316.

[60] Y. Huang, Z. Lin, R. Cao, Palladium nanoparticles encapsulated in a metal–organic framework as efficient heterogeneous catalysts for direct C2 arylation of indoles, Chemistry–A European Journal 17 (2011) 12706-12712.

[61] H.-L. Jiang, B. Liu, T. Akita, M. Haruta, H. Sakurai, Q. Xu, Au@ ZIF-8: CO oxidation over gold nanoparticles deposited to metal− organic framework, J. Am. Chem. Soc. 131 (2009) 11302-11303.

[62] B. Liu, H. Shioyama, T. Akita, Q. Xu, Metal-organic framework as a template for porous carbon synthesis, J. Am. Chem. Soc. 130 (2008) 5390-5391.

[63] Z. Xiang, Z. Hu, D. Cao, W. Yang, J. Lu, B. Han, W. Wang, Metal–organic frameworks with incorporated carbon nanotubes: improving carbon dioxide and methane storage capacities by lithium doping, Angewandte Chemie International Edition 50 (2011) 491-494.

[64] H.-L. Jiang, B. Liu, Y.-Q. Lan, K. Kuratani, T. Akita, H. Shioyama, F. Zong, Q. Xu, From metal–organic framework to nanoporous carbon: toward a very high surface area and hydrogen uptake, J. Am. Chem. Soc. 133 (2011) 11854-11857.

[65] A. Dhakshinamoorthy, H. Garcia, Catalysis by metal nanoparticles embedded on metal–organic frameworks, Chemical Society Reviews 41 (2012) 5262-5284.

[66] P. Serra-Crespo, E.V. Ramos-Fernandez, J. Gascon, F. Kapteijn, Synthesis and characterization of an amino functionalized MIL-101 (Al): Separation and catalytic properties, Chemistry of Materials 23 (2011) 2565-2572.

[67] Y. Zhou, K. Neyerlin, T.S. Olson, S. Pylypenko, J. Bult, H.N. Dinh, T. Gennett, Z. Shao, R. O'Hayre, Enhancement of Pt and Pt-alloy fuel cell catalyst activity and durability via nitrogen-modified carbon supports, Energy & Environmental Science 3 (2010) 1437-1446.

[68] Z. Li, J. Liu, Z. Huang, Y. Yang, C. Xia, F. Li, One-pot synthesis of Pd nanoparticle catalysts supported on N-doped carbon and application in the domino carbonylation, ACS Catalysis 3 (2013) 839-845.

[69] Z. Guo, T. Kobayashi, L.L. Wang, T.W. Goh, C. Xiao, M.A. Caporini, M. Rosay, D.D. Johnson, M. Pruski, W. Huang, Selective Host–Guest Interaction between Metal Ions and Metal–Organic Frameworks Using Dynamic Nuclear Polarization Enhanced Solid-State NMR Spectroscopy, Chemistry–A European Journal 20 (2014) 16308-16313.

[70] J.-K. Sun, Q. Xu, From metal–organic framework to carbon: toward controlled hierarchical pore structures via a double-template approach, Chemical Communications 50 (2014) 13502-13505.

[71] C. Chang, Y. Fu, M. Hu, C. Wang, G. Shan, L. Zhu, Photodegradation of bisphenol A by highly stable palladium-doped mesoporous graphite carbon nitride (Pd/mpg-C 3 N 4) under simulated solar light irradiation, Applied Catalysis B: Environmental 142 (2013) 553-560.

[72] L. Sun, C. Tian, Y. Fu, Y. Yang, J. Yin, L. Wang, H. Fu, Nitrogen-Doped Porous Graphitic Carbon as an Excellent Electrode Material for Advanced Supercapacitors, Chemistry–A European Journal 20 (2014) 564-574.

[73] P. Zhang, Y. Gong, H. Li, Z. Chen, Y. Wang, Solvent-free aerobic oxidation of hydrocarbons and alcohols with Pd@ N-doped carbon from glucose, Nature communications 4 (2013) 1593.

[74] K. Fulajtárova, T. Soták, M. Hronec, I. Vávra, E. Dobročka, M. Omastová, Aqueous phase hydrogenation of furfural to furfuryl alcohol over Pd–Cu catalysts, Applied Catalysis A: General 502 (2015) 78-85.

[75] M. Villaverde, N. Bertero, T. Garetto, A. Marchi, Selective liquid-phase hydrogenation of furfural to furfuryl alcohol over Cu-based catalysts, Catalysis today 213 (2013) 87-92.

[76] M. Shirotori, S. Nishimura, K. Ebitani, One-pot synthesis of furfural derivatives from pentoses using solid acid and base catalysts, Catalysis Science & Technology 4 (2014) 971-978.

[77] E.I. Gürbüz, S.G. Wettstein, J.A. Dumesic, Conversion of hemicellulose to furfural and levulinic acid using biphasic reactors with alkylphenol solvents, ChemSusChem 5 (2012) 383-387.